

# Circulating microRNAs signature correlates with positive [ $^{18}\text{F}$ ]fluorodeoxyglucose-positron emission tomography in patients with abdominal aortic aneurysm



Audrey Courtois, MSc, PhD,<sup>a,b</sup> Betty Nusgens, PhD,<sup>c</sup> Nancy Garbacki, PhD,<sup>c</sup> Roland Hustinx, MD, PhD,<sup>d</sup> Pierre Gomez, MD,<sup>e</sup> Jean-Olivier Defraigne, MD, PhD,<sup>b</sup> Alain C. Colige, PhD,<sup>c</sup> and Natzi Sakalihan, MD, PhD,<sup>a,b</sup> Liège, Belgium

## ABSTRACT

**Background:** Prediction of abdominal aortic aneurysm (AAA) rupture is a challenging issue. Small noncoding microRNAs (miRNAs) are potent regulators of gene expression and are considered as valuable circulating biomarkers. Recently, [ $^{18}\text{F}$ ] fluorodeoxyglucose (FDG) uptake detected by positron emission tomography (PET) in AAA was correlated with cellular and molecular alterations involved in wall instability and its potential rupture. Our study aimed at identifying circulating miRNAs correlated with a positive PET that could help discriminate patients at high risk of rupture.

**Methods:** The level of 372 miRNAs was evaluated by polymerase chain reaction array in plasma from 35 AAA patients displaying no FDG uptake (AO) and 22 patients with a positive PET uptake (A+). The modulated miRNAs were validated by quantitative polymerase chain reaction and measured in aneurysmal tissues from both groups of patients.

**Results:** Six circulating miRNAs were found significantly modulated in A+ vs AO patients. They were significantly correlated not only between them but also with the intensity of FDG uptake. Two of them correlated also with the AAA diameter. These miRNAs displayed significant discriminating power between the A+ and AO groups as determined by receiver operating characteristic curves. Three downregulated circulating miRNAs (miR-99b-5p, miR-125b-5p, and miR-204-5p) were also significantly reduced in the aneurysmal tissue, specifically in the FDG-uptake site, compared with a negative zone in the same aneurysm and with AO aneurysms. They were further significantly inversely correlated with the expression, at the positive uptake site, of some of their potential gene targets, most notably matrix metalloproteinase 13.

**Conclusions:** Six miRNAs were identified as potential new circulating biomarkers of PET+ AAA. Three of these were similarly modulated in the metabolically active aneurysmal wall and might be directly involved in AAA instability. (J Vasc Surg 2018;67:585-96.)

**Clinical Relevance:** Identifying specific biomarkers able to predict rupture is the most challenging facet for management of patients with abdominal aortic aneurysm. We previously demonstrated that uptake of [ $^{18}\text{F}$ ]fluorodeoxyglucose in the aneurysmal wall detected by positron emission tomography-computed tomography was associated with clinical signs presaging rupture and with cellular and molecular alterations indicating active wall remodeling. In this work, we identified six circulating microRNAs significantly correlated with a positive [ $^{18}\text{F}$ ]fluorodeoxyglucose uptake, and three of them were similarly modulated in the metabolically active aneurysmal wall and potentially involved in abdominal aortic aneurysm instability. These microRNAs could represent useful biomarkers to discriminate patients at high risk of rupture and best help with therapeutic decision.

Abdominal aortic aneurysm (AAA) is an asymptomatic dilatation of the infrarenal aorta affecting 4% to 8% of men aged >65 years.<sup>1,2</sup> AAA rupture is fatal in 65% to 80% of cases and is considered as the 13th leading cause of death in industrial countries.<sup>3</sup> Prediction of aneurysm rupture is currently based on its diameter, which is

considered at risk when  $\geq 5.5$  cm. However, because some small AAAs can also rupture<sup>4</sup> and some large aneurysms may stay stable without any sign of rupture, this parameter is not fully reliable.

In previous studies, we and others have demonstrated that a positive uptake of [ $^{18}\text{F}$ ]fluorodeoxyglucose (FDG)

From the Surgical Research Center, Interdisciplinary Cluster for Applied Genoproteomics-Cardiovascular Science Unit,<sup>a</sup> the Department of Cardiovascular and Thoracic Surgery, Centre Hospitalier Universitaire Liège,<sup>b</sup> the Laboratory of Connective Tissues Biology, Interdisciplinary Cluster for Applied Genoproteomics-Research,<sup>c</sup> and the Department of Nuclear Medicine, Centre Hospitalier Universitaire Liège,<sup>d</sup> University of Liège; and the Department of Nuclear Medicine, Centre Hospitalier Chrétien St Joseph.<sup>e</sup>

This work was supported by the European Program FP7 "Fighting aneurysmal diseases" (no. 200647) and by the Aneurysmal Pathology Foundation.

Author conflict of interest: none.

Presented at the Fourth International Meeting on Aortic Diseases, Liège, Belgium, September 11-13, 2014; and at the Arteriosclerosis, Thrombosis and Vascular Biology meeting, San Francisco, Calif, May 7-9, 2015.

Additional material for this article may be found online at [www.jvascsurg.org](http://www.jvascsurg.org).

Correspondence: Audrey Courtois, MSc, PhD, Surgical Research Center (CREDEC), Interdisciplinary Cluster for Applied Genoproteomics-Cardiovascular Unit, University of Liège, Tour de Pathologie, B23/+5, Sart-Tilman B-4000, Belgium (e-mail: [a.courtois@ulg.ac.be](mailto:a.courtois@ulg.ac.be)).

The editors and reviewers of this article have no relevant financial relationships to disclose per the JVS policy that requires reviewers to decline review of any manuscript for which they may have a conflict of interest.

0741-5214

Copyright © 2017 by the Society for Vascular Surgery. Published by Elsevier Inc. <http://dx.doi.org/10.1016/j.jvs.2016.12.112>

detected by positron emission tomography (PET) in the aneurysmal wall was a warning signal associated with a dense inflammatory infiltrate, a loss of smooth muscle cells in the media, and an active remodeling of extracellular matrix that may ultimately lead to wall instability.<sup>5-8</sup> In the same context, English et al<sup>9</sup> demonstrated a relationship between a positive FDG signal and rupture of AAA in an experimental animal model.

A challenging aspect of AAA monitoring is the lack of reliable biomarkers reflecting the progression of aneurysm and the risk of rupture. MicroRNAs (miRNAs) are single-stranded, small noncoding RNAs that post-transcriptionally regulate gene expression by preventing translation or stimulating degradation, or both, of their target messenger RNA. They act as crucial regulators of many physiologic and pathologic processes.<sup>10</sup> Since the discovery of stable circulating miRNAs and their association with lymphoma by Lawrie et al,<sup>11</sup> many studies have correlated defined sets of circulating miRNAs with pathologic conditions,<sup>12,13</sup> notably in cardiovascular diseases.<sup>14,15</sup> A modulation of the expression of some miRNAs has been found in plasma and tissues of human AAA<sup>16</sup> and correlated with their progression in animal models.<sup>17,18</sup>

In this study, the expression of the most abundant plasmatic miRNAs was analyzed in AAA patients presenting (A+) or not (AO) an uptake of FDG to identify miRNAs that could be relevant biomarkers of AAA progression and potential predictors of rupture. The significantly modulated plasmatic miRNAs were also evaluated in the aneurysmal tissue collected from AO and A+ patients at the site of uptake (A<sub>pos</sub>) and at a distant negative site in the same aneurysm (A<sub>neg</sub>). In a previous study, we used transcriptomic analysis to identify a set of genes modulated in this FDG+ uptake site.<sup>7</sup> In the present study, this set of genes was compared with the predicted target genes of the modulated miRNAs to identify relevant signaling pathways.

## METHODS

This project was approved by the Ethics Committee of the University Hospital of Liège, Belgium.

**Patients and acquisition of PET computed tomography images.** PET/computed tomography (CT) data were acquired in two hospitals (Centre Hospitalier Universitaire and Centre Hospitalier Chrétien, Liège, Belgium), using a 16-slice CT Gemini BB (Philips, Best, The Netherlands) or a 16-slice CT Discovery LS (GE Healthcare, Waukesha, Wisc). The image acquisition protocol was previously described.<sup>6</sup>

PET/CT was performed in 57 patients, and two nuclear physicians discriminated patients as AO and A+ based on visual examination of PET/CT images. The standardized uptake value (SUV) of the positive spots was expressed as a ratio (rSUV) between the uptake in the

## ARTICLE HIGHLIGHTS

- **Type of Research:** Prospective experimental study
- **Take Home Message:** MicroRNAs are altered in patients with altered [<sup>18</sup>F]fluorodeoxyglucose signaling on positron emission tomography-computed tomography imaging and may be potential biomarkers for aneurysm growth.
- **Recommendation:** The authors suggest that microRNA may serve as potential biomarkers for identifying patients at risk for aneurysm rupture.

AAA wall and in the liver. The study excluded patients with known connective tissue disorders or thoracoabdominal aortic aneurysms.

**Samples collection.** Plasma samples were collected from 57 patients at the time of the PET/CT examination and stored at  $-80^{\circ}\text{C}$  until use. In a first step, plasma from 41 patients (24 AO and 17 A+) was used for quantitative polymerase chain reaction (qPCR) array, as described below. The study further enrolled 16 patients (11 AO and 5 A+) for validations of the PCR array by qPCR.

Biopsy specimens of aortic tissue were collected during surgery from 12 AO and nine A+ patients. For these nine A+ patients, one biopsy was taken at the site of FDG uptake (A<sub>pos</sub>), localized using anatomic landmarks and CT images, as previously detailed,<sup>6</sup> and a second sample was taken in the same aneurysm at a distant site negative for FDG uptake (A<sub>neg</sub>). Tissue was dissected to separate media and adventitia, snap frozen in liquid nitrogen, and kept at  $-80^{\circ}\text{C}$  until use.

**Purification of miRNA.** Total RNA from plasma was purified using the miRNeasy Plasma/Serum Kit (Qiagen, Valencia, Calif) according to the manufacturer's protocol. Briefly, 1 mL of lysis reagent was added to 200  $\mu\text{L}$  of plasma. Synthetic miR-39 from *Caenorhabditis elegans* (cel-miR-39) was added as a spike-in control for purification efficiency. After addition of chloroform and centrifugation, total RNA was precipitated from the upper aqueous phase by adding 1.5 volumes of 100% ethanol and finally eluted with 14  $\mu\text{L}$  of RNase-free water.

Aneurysmal tissue samples were ground at liquid nitrogen temperature (Dismembrator; B. Braun Biotech International, Melsungen, Germany), and total RNA was extracted as previously described.<sup>7</sup>

**Plasma miRNA PCR array.** Total RNA from 24 AO and 17 A+ plasma samples were pooled into four and three pools, respectively. Pooled RNA was reverse transcribed using the miScript II RT Kit with HiSpec buffer (Qiagen), and the complementary DNA was preamplified with the miScript PreAMP PCR Kit (Qiagen) according to the manufacturer's protocol. The PCR array was performed

on a plate precoated with the primers for the 372 most represented circulating miRNAs (miScript miRNA PCR Array Human Serum/Plasma; Qiagen). Each reaction was normalized by the geometric mean of the cycle threshold (Ct) of each expressed (<35 cycles) miRNA in the plate.<sup>19</sup> The relative expression of each miRNA in the plasma of A+/AO patients was calculated by the  $\Delta\Delta C_t$  method.

**Real-time qPCR.** Real-time qPCR was performed, individually, on RNA samples from 35 AO patients and 22 A+ patients using the miScript SYBR Green PCR Kit (Qiagen), a universal reverse primer (Qiagen), and a specific forward primer for each miRNA (Supplementary Table I, online only). Expression levels of plasmatic miRNAs, using preamplified complementary DNA as described above, were normalized by that of the synthetic cel-miR-39 and expressed relative to the plasmatic level of one patient taken as reference. RNA from tissue samples (600 ng) was reverse transcribed using the miScript II RT Kit (Qiagen), and miRNA expression levels were normalized by the geometric mean of the expression of miR-16 and a stable small noncoding RNA, SNORD95 (small nucleolar RNA, C/D box 95). The  $\Delta\Delta C_t$  method was used to calculate the fold change of each miRNA as the difference between the median values obtained for A+ and AO tissues converted to linear form by the  $2^{-\Delta\Delta C_t}$  method taking the PCR reaction efficiency into account (Supplementary Table I, online only).

**Bioinformatics analysis.** Target genes were predicted for the modulated using the miRNA target prediction databases TargetScan, PicTar, and miRTarBase. Potential modulated pathways were analyzed using the ToppGene software.<sup>20</sup> The predicted targets for miR-99b-5p, miR-125b-5p, and miR-204-5p were compared with the list of modulated genes in the A+<sub>pos</sub> site compared with the A+<sub>neg</sub> site determined in our previous transcriptomic study.<sup>7</sup>

**Statistical analysis.** Results are expressed as the median with the interquartile range (25-75 percentile) and considered to be significant at the 5% critical level ( $P < .05$ ) by using the Mann-Whitney *U* test for unpaired samples or the Wilcoxon test for paired samples. Receiver-operator characteristics (ROC) curve and the area under the curve (AUC) were established using GraphPad Prism software (GraphPad Software, Inc, La Jolla, Calif). Correlations between modulated miRNA and rSUV and AAA diameter and expression of selected genes were established using the Spearman test for nonparametric values.

## RESULTS

**PET/CT data, patient demographics, and clinical features.** The metabolic activity in the AAA expressed as the rSUV (SUV AAA/SUV liver) was determined for the

**Table I.** Characteristics of abdominal aortic aneurysm (AAA) patients with no [<sup>18</sup>F]fluorodeoxyglucose (FDG) uptake (AO) and with a positive FDG uptake (A+)

| Patient characteristics <sup>a</sup> | AO (n = 35)      | A+ (n = 22)                   |
|--------------------------------------|------------------|-------------------------------|
| Age, years                           | 74 (68-79)       | 75 (68-81)                    |
| Gender distribution                  |                  |                               |
| Male                                 | 35               | 20                            |
| Female                               | 0                | 2                             |
| Aneurysm diameter, mm                | 54 (50-62)       | 55 (51-59)                    |
| ≤50 mm                               | 10               | 5                             |
| rSUV <sup>b</sup>                    | 0.43 (0.35-0.62) | 0.96 (0.87-1.09) <sup>c</sup> |
| ≤50 mm                               | 0.59 (0.45-0.78) | 1.17 (1.00-1.38) <sup>d</sup> |
| >50 mm                               | 0.41 (0.35-0.58) | 0.91 (0.84-1.03) <sup>c</sup> |
| Cardiovascular events                | 20               | 9                             |
| Hypertension                         | 22               | 14                            |
| Smokers                              |                  |                               |
| Current                              | 12               | 7                             |
| Former                               | 20               | 12                            |
| COPD                                 | 16               | 7                             |
| Diabetes                             | 3                | 5                             |
| Hyperlipidemia                       | 23               | 13                            |
| Medication                           |                  |                               |
| Statins                              | 19               | 12                            |
| β-Blocker                            | 11               | 6                             |
| Calcium channel blocker              | 4                | 4                             |
| ACEI                                 | 4                | 2                             |
| NSAID                                | 0                | 1                             |

ACEI, Angiotensin converting enzyme inhibitor; COPD, chronic obstructive pulmonary disease; NSAID, non-steroidal anti-inflammatory drug; SUV, standard uptake value.  
<sup>a</sup>Continuous data are shown as median (25-75 interquartile range), and categorical data as number.  
<sup>b</sup>Ratio of SUV AAA/SUV liver.  
<sup>c</sup> $P < .001$  Mann-Whitney *U* test.  
<sup>d</sup> $P < .01$ .

57 patients enrolled in the study (Table I). Uptake of FDG in 22 patients appeared as focal positive zones in the aneurysmal wall (A+), and 35 patients did not show any positive spots (AO). Men predominated in each group, and no significant difference in the median age was noted between the groups (Table I). Among the 57 patients, 15 had an aneurysm with a diameter ≤50 mm, 10 of them being AO (28%) and five being A+ (23%). The SUV values were significantly higher in the A+ patients and similarly increased in the small and large aneurysm in agreement with the lack of significant correlation between AAA diameter and rSUV in the full cohort (data not shown).

**Modulation of miRNAs level in the plasma of AAA patients.** The expression level of 372 miRNAs was evaluated by a using a miRNA PCR array on four pools of plasmatic RNA from AO patients and three pools from A+ patients. Among the detected miRNAs, 17 were

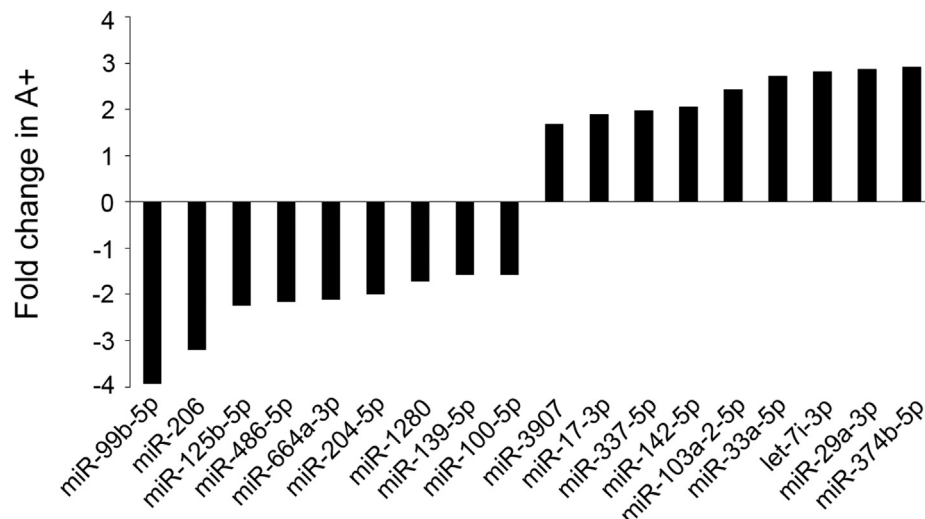


**Fig 1.** Circulating microRNAs (miRNAs) modulated in patients with aneurysms displaying positive [ $^{18}\text{F}$ ]fluorodeoxyglucose (FDG) uptake (A+) on positron emission tomography (PET) compared with patients displaying no uptake (A0) were measured by polymerase chain reaction (PCR) array. Seventeen miRNAs are modulated in the three pools of plasmatic RNA from 17 A+ patients compared with the four pools of RNA from 24 A0 patients. Nine are downregulated and eight are upregulated. Results are expressed as the fold-change relative to the median of miRNAs expression in the A0 pools.  $P < .05$  by Mann-Whitney  $U$  test.

modulated in the A+ pools (fold induction  $>1.5$ ;  $P < .05$ ) compared with the A0, nine being downregulated and eight upregulated (Fig 1). Validations were performed by real-time qPCR on the plasma of each patient (A0,  $n = 35$ ; A+,  $n = 22$ ) for nine miRNAs selected among those displaying the highest fold changes. High correlations with the PCR array results were obtained for all selected miRNAs except for miR-374b-5p, which was therefore excluded from the study for further analyses (Supplementary Table II, online only). Six miRNAs were significantly modulated in A+ patients compared with the A0 group: four were downregulated (miR-99b-5p, miR-125b-5p, miR-204-5p, and miR-486-5p), and two were upregulated (miR-33a-5p and miR-142-5p; Fig 2, A). The four downregulated miRNAs were significantly correlated between them, and the two upregulated miRNAs were significantly negatively correlated with miR-486-5p (Fig 2, B).

Correlations between the expression level of these six miRNAs and the uptake of FDG expressed by the maximum SUV in the AAA, the rSUV (AAA/liver) and the aneurysm diameter were evaluated (Table II). The four downregulated miRNAs and the two upregulated miRNAs were significantly and, respectively, negatively and positively correlated with the rSUV (Table II). All of them were also correlated with the maximum SUV except miR-142-5p. Only miR-125b-5p and miR-486-5p were negatively correlated with the aneurysmal diameter. The suitability of these six modulated miRNAs to discriminate unstable from stable aneurysms was investigated by calculating their specificity and sensitivity and establishing ROC curves. The AUC was  $>0.75$  for the four

downregulated miRNAs, indicating their potential value as biomarkers of a PET+ aneurysm (Fig 3).

**Bioinformatic analysis of potential targets of the six circulating validated miRNAs.** Potential targets for the six modulated miRNAs were explored using three different databases: TargetScan, PicTar, and miRTarBase (direct links are available in Appendix Files 1 to 6, online only). The search found  $\sim 1000$  target genes for miR-125b-5p, miR-142-5p, and miR-204,  $\sim 600$  targets genes for miR-33a-5p, and 100 genes for miR-99b-5p and miR-486-5p. The lists of potential target genes were used to select biological pathways using the ToppGene software (Supplementary Table III, online only). No pathway was obtained for miR-99b-5p and miR-486-5p because of the low number of known target genes, but miR-04 seems to participate to neuronal pathways that do not seem relevant to this study. MiR-125b-5p is more directly linked to intracellular pathways involved in ubiquitous processes such as mitogen-activated protein kinase signalling. Finally, the transforming growth factor (TGF)- $\beta$  pathway is known to be regulated by miR-33a-5p and by miR-142-5p which might also target different SMAD, TGF- $\beta 2$ , and TGF- $\beta$  receptors.

**Modulation of miRNAs expression in the AAA wall of A+ patients.** The expression of the six miRNAs modulated in the plasma of A+ patients was measured in the aneurysmal wall, separately in adventitia and media, from 12 A0 and nine A+ patients both at the FDG uptake site (A+<sub>pos</sub>) and at a distant negative site from the same aneurysm (A+<sub>neg</sub>). In adventitia, the expression of these miRNAs

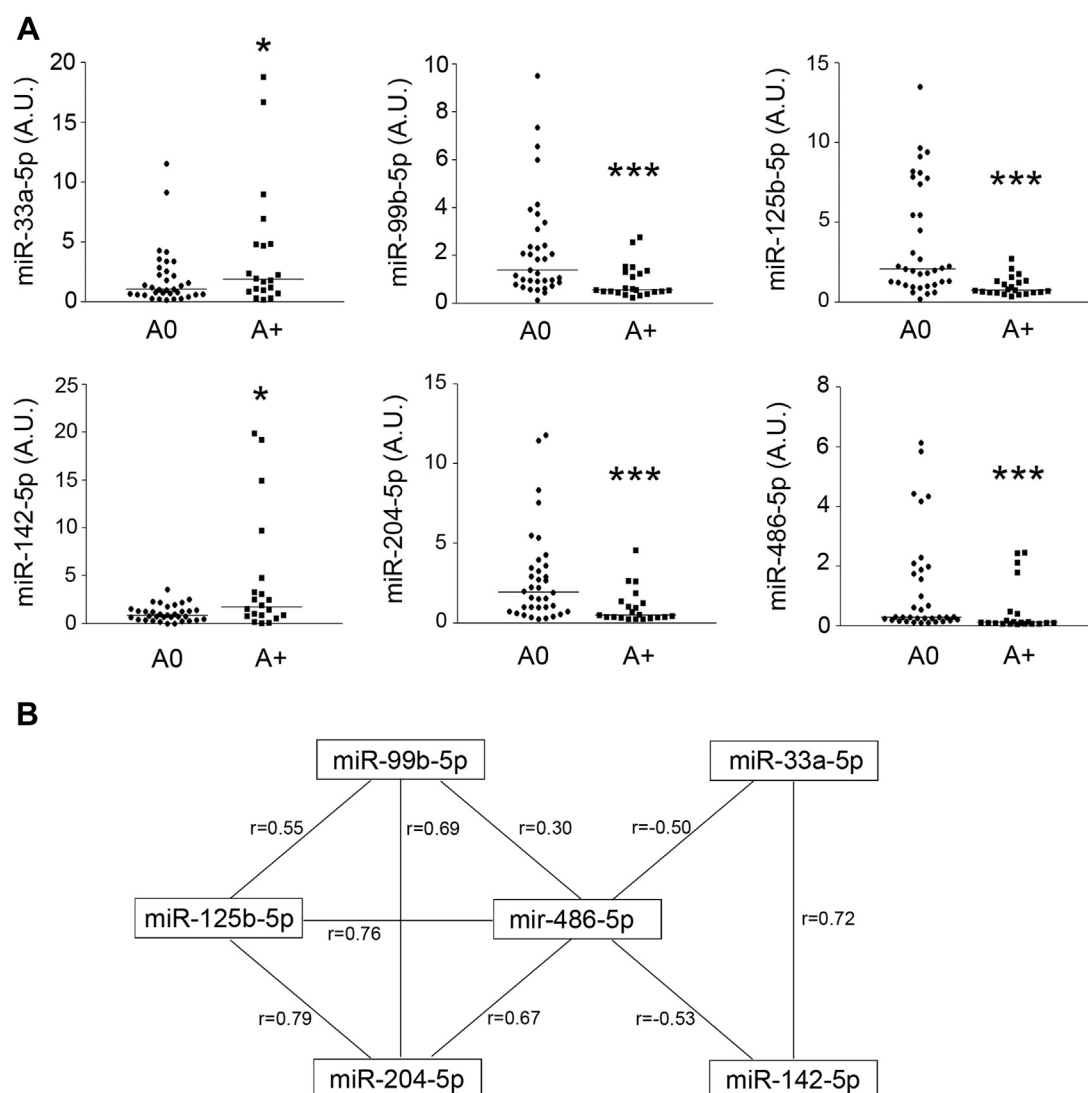


**Fig 2.** Expression of the six circulating microRNAs (miRNAs) validated in patients with aneurysms displaying no [ $^{18}\text{F}$ ]fluorodeoxyglucose (FDG) uptake (A0) and those positive (A+) on positron emission tomography (PET). **A**, The expression of each miRNA in arbitrary units (A.U.) was measured individually in A0 ( $n = 35$ ) and A+ patients ( $n = 22$ ). The median is shown for each group. \* $P < .05$  and \*\*\* $P < .001$  by Mann-Whitney  $U$  Test. **B**, Significant correlations were found between miRNAs established by using the Spearman test for nonparametric samples ( $P < .05$ ).

was very low compared with the media. Moreover, given the high heterogeneity of cells population in the adventitia between patients, the normalization and the quantification of miRNAs were not reliable. In the media, miR-99b-5p, miR-125b-5p, and miR-204-5p were significantly downregulated in the A+<sub>pos</sub> site compared with its negative counterpart and also with A0 patients (Fig 4).

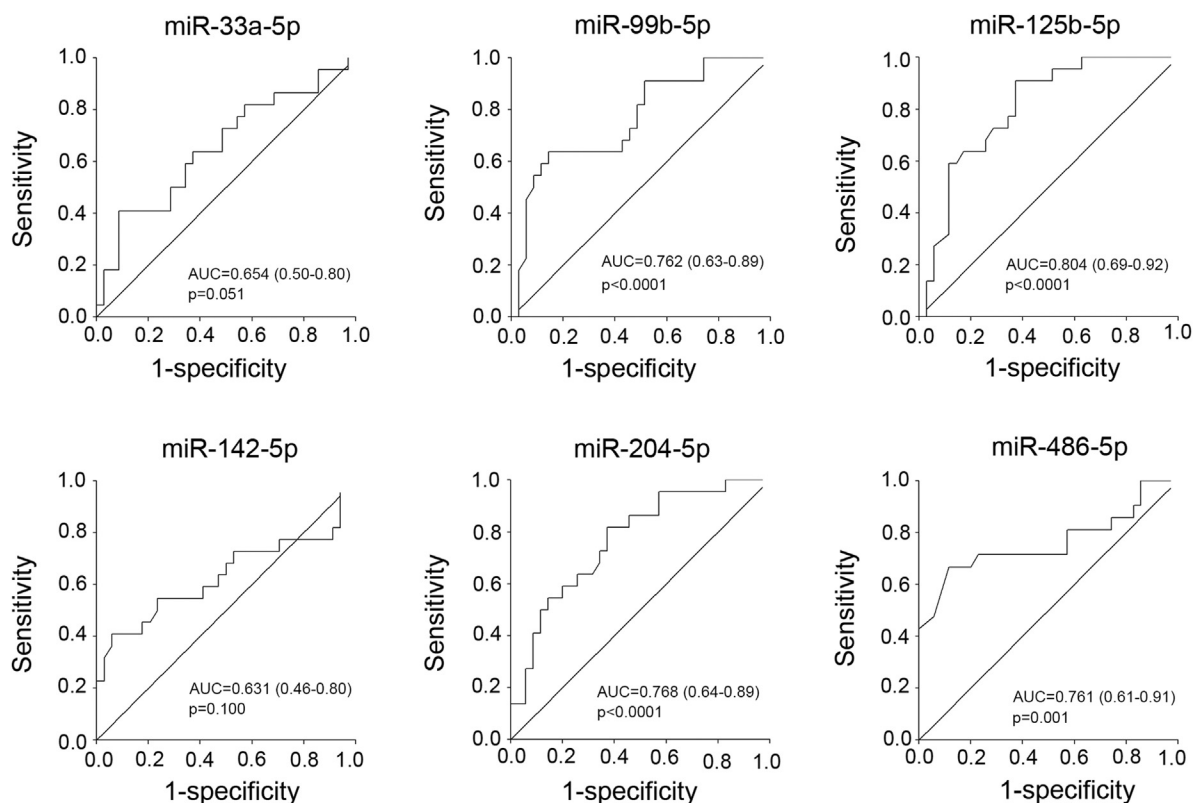
**Potential targets of modulated miRNAs in correlation with the transcriptomic study in A+ media.** As highlighted in the summarizing Table III, downregulation of miR-99b-5p, miR-125b-5p, and miR-204-5p appears to be specifically associated with FDG uptake and weakening of the aneurysmal wall. To consolidate their role, we compared the validated and potential targets

of these three miRNAs with the set of upregulated genes identified in a previous transcriptomic analysis of the aneurysmal wall from A+ patients.<sup>7</sup> No common genes were obtained for the miR-99b-5p whereas ~30 targets genes were found to be modulated in our transcriptomic study for miR-125b-5p and miR-204-5p (Fig 5).<sup>7,21</sup> Runt-related transcription factor 2 (RUNX2), a transcription factor involved in osteochondral development, is a validated target of miR-204-5p. Most interestingly, matrix metalloproteinase (MMP) 13, an enzyme involved in endochondral development and pathologic remodeling in cancer and arthritis, was significantly increased in the A+<sub>pos</sub> sites of aneurysmal wall. This potent collagenase is a validated target of miR-125b-5p (Fig 5). It was also found here significantly



**Table II.** Correlations between circulating microRNAs (*miRNAs*) and the maximum standard uptake value (*SUV max*), ratio of SUV (*rSUV*) in abdominal aortic aneurysm (AAA)/liver, and diameter of the AAA<sup>a</sup>

| miRNA       | SUV max AAA |                   | rSUV AAA/liver |                   | AAA diameter |                   |
|-------------|-------------|-------------------|----------------|-------------------|--------------|-------------------|
|             | r           | P                 | r              | P                 | R            | P                 |
| miR-33a-5p  | +0.313      | .01 <sup>b</sup>  | +0.258         | .03 <sup>b</sup>  | +0.173       | .105              |
| miR-99b-5p  | −0.267      | .022 <sup>b</sup> | −0.251         | .03 <sup>b</sup>  | −0.118       | .19               |
| miR-125b-5p | −0.392      | .002 <sup>c</sup> | −0.365         | .003 <sup>c</sup> | −0.278       | .018 <sup>b</sup> |
| miR-142-5p  | +0.179      | .091              | +0.242         | .035 <sup>b</sup> | −0.138       | .153              |
| miR-204-5p  | −0.277      | .018 <sup>b</sup> | −0.279         | .018 <sup>b</sup> | −0.22        | .05               |
| miR-486-5p  | −0.336      | .006 <sup>c</sup> | −0.29          | .015 <sup>b</sup> | −0.269       | .023 <sup>b</sup> |

<sup>a</sup>Correlations were established with the Spearman test for nonparametric samples (n = 57).<sup>b</sup>P < .05.<sup>c</sup>P < .01.**Fig 3.** Receiver-operator characteristics (ROC) curves analysis was performed each of the six modulated microRNA (miRNAs). The area under the curve (AUC) with the confidence intervals and the P value are shown.

and negatively correlated not only with the expression of miR-125b-5p, as expected, but also with miR-204-5p in the media (Fig 6). Finally, these two miRNAs have in common five potential targets previously found to be upregulated in the A<sub>pos</sub> site, including hyaluronan and proteoglycan link protein 1 (HAPLN1), which is also involved in the formation of cartilaginous matrix (Fig 5).

## DISCUSSION

For the last 15 years, our department has aimed to evaluate the benefit of PET/CT in the management of AAA

patients to improve the discrimination between stable aneurysms and those at high risk of rupture.<sup>5,22</sup> This concept was followed by others who also observed a relationship between uptake of FDG in the aneurysmal wall and inflammation and expression of MMPs in human and rupture in animal models.<sup>8,9</sup> In our cohort of patients, the rSUV did not correlate with the AAA diameter, an observation that was further supported by the similar percentage of small aneurysms ( $\leq 50$  mm) in A0 and A+ patients, suggesting that uptake of FDG is independent of the aneurysm diameter.

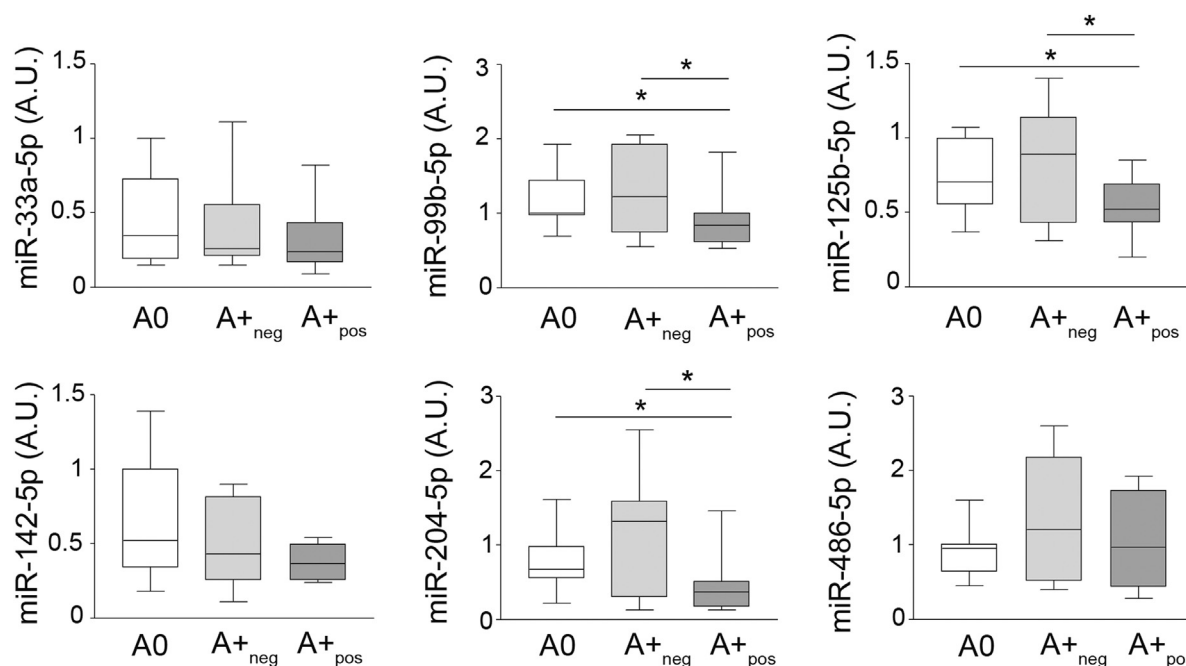


**Fig 4.** Expression of the six modulated microRNAs (miRNA) in the media of aneurysms of 12 patients displaying no [ $^{18}\text{F}$ ]fluorodeoxyglucose (FDG) uptake (A0) and in nine patients positive (A+) on positron emission tomography (PET) at the negative (A+<sub>neg</sub>) and positive (A+<sub>pos</sub>) site. A.U., Arbitrary units. \* $P \leq .05$  by the Mann-Whitney  $U$  test for unpaired samples and with the Wilcoxon test for paired samples. The horizontal line in the middle of each box indicates the median; the top and bottom borders of the box mark the 75th and 25th percentiles, respectively, and the whiskers above and below the box extend 1.5 interquartile range in either direction.

**Table III.** Summary of microRNAs (miRNAs) modulations in plasma and in tissue samples

| miRNA         | Plasma   |                                 | Tissue                  |                         |  |
|---------------|----------|---------------------------------|-------------------------|-------------------------|--|
|               | A+ vs A0 | Correlation vs rSUV vs diameter | A+ <sub>neg</sub> vs A0 | A+ <sub>pos</sub> vs A0 | A+ <sub>pos</sub> vs A+ <sub>neg</sub> |
| miR-103a-2-5p | NS       |                                 |                         |                         |  |
| miR-206       | NS       |                                 |                         |                         |  |
| miR-33a-5p    | ↑        | ✓                               | NS                      | NS                      | NS                                     |
| miR-142-5p    | ↑        | ✓                               | NS                      | NS                      | NS                                     |
| miR-204-5p    | ↓↓↓      | ✓                               | NS                      | ↓                       | ↓                                      |
| miR-125b-5p   | ↓↓↓      | ✓                               | NS                      | ↓                       | ↓                                      |
| miR-99b-5p    | ↓↓↓      | ✓                               | NS                      | ↓                       | ↓                                      |
| miR-486-5p    | ↓↓↓      | ✓                               | NS                      | NS                      | NS                                     |

A0, Patients with no [ $^{18}\text{F}$ ]fluorodeoxyglucose uptake; A+, patients with positive FDG uptake; A+<sub>neg</sub>, sample from a negative site in the A+ aneurysm; A+<sub>pos</sub>, sample from a positive site in the A+ aneurysm; NS, not significant; ↑, significantly increased expression,  $P < .05$ ; ↓, significantly decreased expression,  $P < .05$ ; ↓↓↓, significantly decreased expression,  $P < .001$ ; ✓, significant correlation with the standard uptake value ratio (rSUV) in abdominal aortic aneurysm (AAA)/liver or aneurysm diameter by using the Spearman test for nonparametric samples.

PET/CT is, however, an expensive imaging technique and alternative methods, less expensive, noninvasive, and correlated with PET positivity, would need to be developed to detect and follow-up patients at risk. Circulating small miRNAs are now considered as relevant biomarkers of different diseases, notably in cardiovascular diseases.<sup>14</sup>

To facilitate this Discussion, a summary of our results is presented in Table III. Our strategy was first to identify circulating miRNAs differentially expressed in AAA patients presenting with a metabolically active aneurysm, as detected by FDG uptake (A+) or no uptake (A0). Six validated circulating miRNAs were significantly modulated in A+ compared with A0 patients.

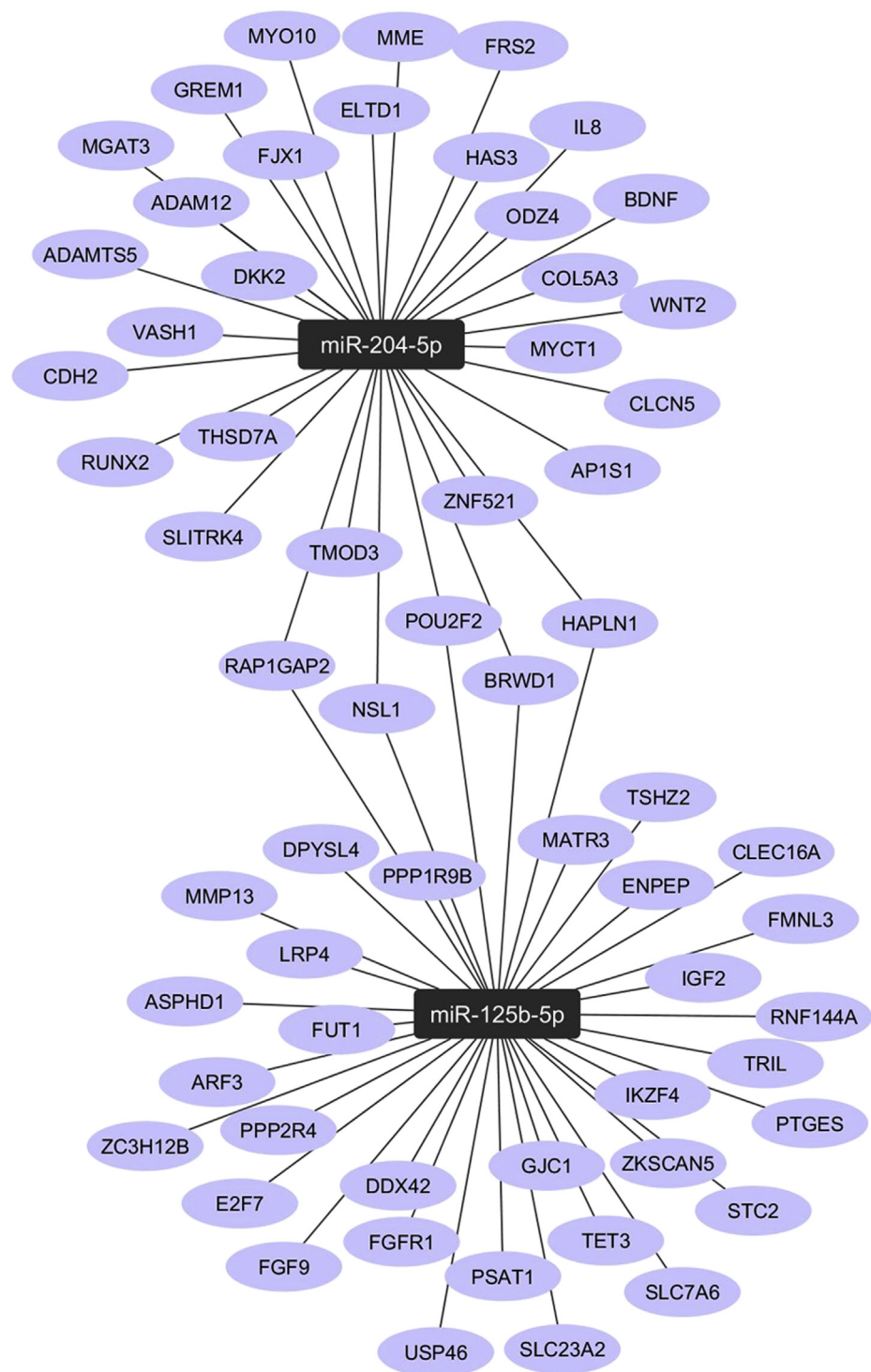


**Fig 5.** Network of miR-204-5p and miR-125b-5p and their validated or potential target genes upregulated in patients with an aneurysm positive [<sup>18</sup>F]fluorodeoxyglucose (FDG) uptake (A+) on positron emission tomography (PET) at the positive (A+<sub>pos</sub>) compared with negative (A+<sub>neg</sub>) site in the media as reported in our previous transcriptomic study.<sup>7</sup> The network was generated using Cytoscape software.<sup>21</sup>

The six identified miRNAs were significantly correlated with the rSUV, and miR-125b-5p and miR-486-5p were also correlated with the AAA diameter.

The approach that we used here is different from the few studies on circulating miRNAs reported in the literature, which usually identify differentially expressed



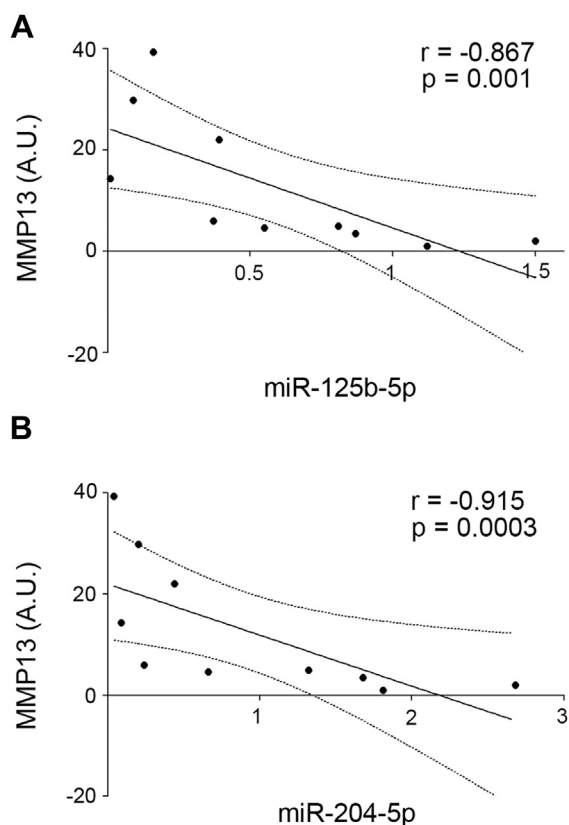


**Fig 6.** Correlations between matrix metalloproteinase (MMP) 13 expression and miR-125b-5p or miR-204-5p level in the media of patients with an aneurysm positive (A+) for [ $^{18}$ F]fluorodeoxyglucose (FDG) uptake on positron emission tomography (PET). A very significant correlation between (A) MMP13 expression and the miR-125b-5p and (B) the miR-204-5p level in 10 samples (5 A<sub>neg</sub> and 5 A<sub>pos</sub>) was established with the Spearman rank test for nonparametric samples. Regression curves (solid line) and the 95% confidence intervals (dotted lines) are shown.

miRNAs by AAA patients, altogether, vs healthy controls. This may explain why none of the circulating miRNAs that we described have been reported elsewhere and further points to their specificity related to metabolic activation of the aneurysmal wall in A+ patients. The discriminating power of the identified miRNAs, as determined by ROC curve analyses, suggests their potential to identify unstable aneurysms in AAA patients, and miR-125b-5p seems the most powerful based on the ROC results (AUC = 0.80;  $P < .0001$ ).

Circulating miRNAs may originate from blood cells that produce exosomes containing miRNAs<sup>23</sup> or from the aneurysmal tissue itself. MiR-125b-5p has been reported to be produced by macrophages<sup>24</sup> and also by cluster of differentiation (CD) 4+ T cells<sup>25</sup> which are the most represented inflammatory cells in the aneurysmal wall.<sup>26</sup> In T cells, miR-125b-5p regulates genes involved

in the differentiation of naïve CD4+ cells.<sup>25</sup> Two other circulating miRNAs modulated in A+ patients, miR-99b-5p and miR-142-5p, were also detected in inflammatory cells, preferentially in monocytes.<sup>27,28</sup>

The identified circulating miRNAs have been previously reported to be modulated in different pathologic condition, for example, miR-486-5p, which is associated with asthma<sup>29</sup> and with acute myocardial infarction,<sup>30,31</sup> or in physiologic processes such as miR-33a-5p involvement in cholesterol homeostasis.<sup>32</sup> Bioinformatic analyses identified a few pathways that could be potentially modulated by these miRNAs. The two upregulated miRNA, miR-33a-5p and miR-142-5p, were reported to inhibit the TGF- $\beta$  pathway, notably by targeting SMAD family members. A major observation in our transcriptomic analysis of the aneurysmal tissue was a significant reduction of TGF- $\beta$  in the media in the A<sub>pos</sub> site. That TGF- $\beta$  overexpression was able to protect the development of AAA in animal models was also demonstrated.<sup>33</sup> MiR-142-5p is largely expressed in atherosclerotic plaques and is involved in the regulation of macrophage apoptosis by targeting TGF- $\beta$ .<sup>34</sup>

The second approach that we used to support our results was to investigate the expression of these six miRNAs in biopsy specimens of AAA wall from AO patients and from A+ patients at the specific positive uptake site (A<sub>pos</sub>) and at a negative distant site (A<sub>neg</sub>). This original approach allows the analysis of samples in the same background, with patients acting their own control. As explained in the Results, only the media could be investigated due to the very low level of expressed miRNAs in the adventitia and the difficulty in normalizing the real-time qPCR results. Three miRNAs (miR-99b-5p, miR-125b-5p, and miR-204-5p) were significantly downregulated in the A<sub>pos</sub> compared with the corresponding A<sub>neg</sub> in the media. These miRNAs were also significantly downregulated in the A<sub>pos</sub> compared with AO samples, demonstrating their specific role in the progression of unstable wall. Pahl et al<sup>17</sup> also found miR-204-5p was downregulated in the aortic wall of AAA patients.

AAA is an inflammatory disease characterized by an overexpression of various cytokines and MMPs during its progression. The observed downregulation of miRNAs in the wall would indeed explain the overexpression of these factors involved in the wall weakening. MMP13, a collagenase involved in chronic inflammatory diseases,<sup>35</sup> was identified as a target for miR-125b-5p in carcinoma cells.<sup>36</sup> We demonstrated in our previous work a large increase of MMP13 expression at the specific site of FDG uptake in the aneurysm.<sup>6</sup> This study found a negative and significant correlation between the expression of MMP13 and the expression of miR-125b-5p and miR-204-5p in the media of A+ patients, which strengthens

the hypothesis that MMP13 messenger RNA might be one of their targets. Significant negative correlation was also found with the expression of MMP1 in the media (data not shown). MMP1 has not been validated as a target of these two miRNAs; however, it might reflect an indirect regulation. These observations are highly relevant to the risk of rupture because collagen degradation by MMPs seems to be the ultimate event preceding the rupture.

Further to its remodeling, the quality of the extracellular matrix might be profoundly altered in A+ wall, as also suggested by our previous transcriptomic study.<sup>7</sup> A series of genes involved in osteochondrogenesis was indeed largely increased in the A+<sub>pos</sub> site, suggesting a switching of the wall cells toward a cartilaginous phenotype and production of a more rigid and incompetent vascular extracellular matrix. Modifications of miR-125b-5p level have been involved in arterial calcification by smooth muscle cells<sup>37</sup> by regulating their transdifferentiation into osteoblast-like cells through the regulation of SP7 and RUNX2,<sup>36</sup> a marker of osteogenesis also found to be involved in arterial calcification.<sup>38,39</sup> MiR-204-5p also directly targets RUNX2. Five other target genes were found to be common between both miRNAs, including HAPLN1, an extracellular matrix protein interacting with proteoglycans and involved in cartilage development.<sup>40</sup> Among the genes involved in the formation of osteochondral matrix found modulated in our previous transcriptomic study, COL11A1 (alpha chain of collagen XI) was also largely increased at FDG-positive sites. Even though this gene was not found to be a potential target of miR-125b-5p or miR-204-5p, negative significant correlations were established between its expression and both miRNAs in the media (data not shown), suggesting that its expression might be indirectly modulated.

## CONCLUSIONS

We have identified six circulating miRNAs modulated in patients with a positive FDG-PET in the aneurysmal wall. This signature might be associated with instability of the wall. Our results also suggest a potential role of miR-125b-5p and miR-204-5p in the progression of aneurysm: their downregulation could allow the ectopic expression of proteins related to cartilaginous extracellular matrix, which does not possess biomechanical properties adapted to elastic tissues and might further induce the overexpression of MMPs involved in aortic wall degradation.

Although three databases using different software and algorithms were used here to predict target genes of miRNAs, some relevant genes might have been overlooked. We are aware that the miRNAs signature reported in this study does not allow by itself a strict discrimination between AO and A+ patients. The results are, however, promising and deserve to be

complemented in studies combining the biomarkers found here with other biomarkers, such as MMPs, on a larger number of patients.

We thank the surgeons and nurses of the Department of Cardiovascular and Thoracic Surgery of the Centre Hospitalier Universitaire of Liège for their contribution to the collection of abdominal aortic aneurysm specimens. We are also grateful to the nurses from the Department of Nuclear Medicine of the Centre Hospitalier Universitaire of Liège and of the Centre Hospitalier Chrétien St Joseph for their help in collecting blood samples.

## AUTHOR CONTRIBUTIONS

Conception and design: AC, BN, NG, JD, ACC, NS

Analysis and interpretation: AC, BN, NG, ACC

Data collection: AC, RH, PG

Writing the article: AC, NG, ACC, NS

Critical revision of the article: BN, NG, RH, PG, JD, ACC, NS

Final approval of the article: AC, BN, NG, RH, PG, JD, ACC, NS

Statistical analysis: AC

Obtained funding: AC, ACC, NS

Overall responsibility: AC

## REFERENCES

1. Lindholt JS, Juul S, Fasting H, Henneberg EW. Screening for abdominal aortic aneurysms: single centre randomised controlled trial. *BMJ* 2005;330:750.
2. Ashton HA, Gao L, Kim LG, Druce PS, Thompson SG, Scott RA. Fifteen-year follow-up of a randomized clinical trial of ultrasonographic screening for abdominal aortic aneurysms. *Br J Surg* 2007;94:696-701.
3. Sakalihasan N, Limet R, Defawe OD. Abdominal aortic aneurysm. *Lancet* 2005;365:1577-89.
4. Powell JT, Gotensparre SM, Sweeting MJ, Brown LC, Fowkes FG, Thompson SG. Rupture rates of small abdominal aortic aneurysms: a systematic review of the literature. *Eur J Vasc Endovasc Surg* 2011;41:2-10.
5. Sakalihasan N, Van Damme H, Gomez P, Rigo P, Lapiere CM, Nusgens B, et al. Positron emission tomography (PET) evaluation of abdominal aortic aneurysm (AAA). *Eur J Vasc Endovasc Surg* 2002;23:431-6.
6. Courtois A, Nusgens BV, Hustinx R, Namur G, Gomez P, Somja J, et al. 18F-FDG uptake assessed by PET/CT in abdominal aortic aneurysms is associated with cellular and molecular alterations prefacing wall deterioration and rupture. *J Nucl Med* 2013;54:1740-7.
7. Courtois A, Nusgens BV, Hustinx R, Namur G, Gomez P, Kuivaniemi H, et al. Gene expression study in positron emission tomography-positive abdominal aortic aneurysms identifies CCL18 as a potential biomarker for rupture risk. *Mol Med* 2014;20:697-706.
8. Reeps C, Essler M, Pelisek J, Seidl S, Eckstein HH, Krause BJ. Increased 18F-fluorodeoxyglucose uptake in abdominal aortic aneurysms in positron emission/computed tomography is associated with inflammation, aortic wall instability, and acute symptoms. *J Vasc Surg* 2008;48:417-23; discussion: 424.

9. English SJ, Piert MR, Diaz JA, Gordon D, Ghosh A, D'Alecy LG, et al. Increased 18F-FDG uptake is predictive of rupture in a novel rat abdominal aortic aneurysm rupture model. *Ann Surg* 2015;261:395-404.
10. Williams AE. Functional aspects of animal microRNAs. *Cell Mol Life Sci* 2008;65:545-62.
11. Lawrie CH, Gal S, Dunlop HM, Pushkaran B, Liggins AP, Pulford K, et al. Detection of elevated levels of tumour-associated microRNAs in serum of patients with diffuse large B-cell lymphoma. *Br J Haematol* 2008;141:672-5.
12. Chen X, Ba Y, Ma L, Cai X, Yin Y, Wang K, et al. Characterization of microRNAs in serum: a novel class of biomarkers for diagnosis of cancer and other diseases. *Cell Res* 2008;18:997-1006.
13. Gilad S, Meiri E, Yogev Y, Benjamin S, Lebanony D, Yerushalmi N, et al. Serum microRNAs are promising novel biomarkers. *PLoS One* 2008;3:e3148.
14. Tijssen AJ, Pinto YM, Creemers EE. Circulating microRNAs as diagnostic biomarkers for cardiovascular diseases. *Am J Physiol Heart Circ Physiol* 2012;303:H1085-95.
15. Kinet V, Halkein J, Dirx E, Windt LJ. Cardiovascular extracellular microRNAs: emerging diagnostic markers and mechanisms of cell-to-cell RNA communication. *Front Genet* 2013;4:214.
16. Stather PW, Sylvius N, Sidloff DA, Dattani N, Verissimo A, Wild JB, et al. Identification of microRNAs associated with abdominal aortic aneurysms and peripheral arterial disease. *Br J Surg* 2015;102:755-66.
17. Pahl MC, Derr K, Gabel G, Hinterseher I, Elmore JR, Schworer CM, et al. MicroRNA expression signature in human abdominal aortic aneurysms. *BMC Med Genomics* 2012;5:25.
18. Maegdefessel L, Azuma J, Tsao PS. MicroRNA-29b regulation of abdominal aortic aneurysm development. *Trends Cardiovasc Med* 2014;24:1-6.
19. Mestdagh P, Van Vlierberghe P, De Weer A, Muth D, Westermann F, Speleman F, et al. A novel and universal method for microRNA RT-qPCR data normalization. *Genome Biol* 2009;10:R64.
20. Chen J, Bardes EE, Aronow BJ, Jegga AG. ToppGene Suite for gene list enrichment analysis and candidate gene prioritization. *Nucleic Acids Res* 2009;37(Web Server issue):W305-11.
21. Shannon P, Markiel A, Ozier O, Baliga NS, Wang JT, Ramage D, et al. Cytoscape: a software environment for integrated models of biomolecular interaction networks. *Genome Res* 2003;13:2498-504.
22. Defawe OD, Hustinx R, Defraigne JO, Limet R, Sakalihasan N. Distribution of F-18 fluorodeoxyglucose (F-18 FDG) in abdominal aortic aneurysm: high accumulation in macrophages seen on PET imaging and immunohistology. *Clin Nucl Med* 2005;30:340-1.
23. Pritchard CC, Kroh E, Wood B, Arroyo JD, Dougherty KJ, Miyaji MM, et al. Blood cell origin of circulating microRNAs: a cautionary note for cancer biomarker studies. *Cancer Prev Res* 2012;5:492-7.
24. Chaudhuri AA, So AY, Sinha N, Gibson WS, Taganov KD, O'Connell RM, et al. MicroRNA-125b potentiates macrophage activation. *J Immunol* 2011;187:5062-8.
25. Rossi RL, Rossetti C, Wenandy L, Curti S, Ripamonti A, Bonnal RJ, et al. Distinct microRNA signatures in human lymphocyte subsets and enforcement of the naive state in CD4+ T cells by the microRNA miR-125b. *Nat Immunol* 2011;12:796-803.
26. Galle C, Schandene L, Stordeur P, Peignois Y, Ferreira J, Wautrecht JC, et al. Predominance of type 1 CD4+ T cells in human abdominal aortic aneurysm. *Clin Exp Immunol* 2005;142:519-27.
27. Leidinger P, Backes C, Dahmke IN, Galata V, Huwer H, Stehle I, et al. What makes a blood cell based miRNA expression pattern disease specific?—a miRNome analysis of blood cell subsets in lung cancer patients and healthy controls. *Oncotarget* 2014;5:9484-97.
28. Bidzhekov K, Gan L, Denecke B, Rostalsky A, Hristov M, Koeppl TA, et al. microRNA expression signatures and parallels between monocyte subsets and atherosclerotic plaque in humans. *Thromb Haemost* 2012;107:619-25.
29. Wang Y, Yang L, Li P, Huang H, Liu T, He H, et al. Circulating microRNA signatures associated with childhood asthma. *Clin Lab* 2015;61:467-74.
30. Zhang R, Lan C, Pei H, Duan G, Huang L, Li L. Expression of circulating miR-486 and miR-150 in patients with acute myocardial infarction. *BMC Cardiovasc Disord* 2015;15:51.
31. Toivonen JM, Manzano R, Olivan S, Zaragoza P, Garcia-Redondo A, Osta R. MicroRNA-206: a potential circulating biomarker candidate for amyotrophic lateral sclerosis. *PLoS One* 2014;9:e89065.
32. Rayner KJ, Suarez Y, Davalos A, Parathath S, Fitzgerald ML, Tamehiro N, et al. MiR-33 contributes to the regulation of cholesterol homeostasis. *Science* 2010;328:1570-3.
33. Dai J, Losy F, Guinault AM, Pages C, Anegon I, Desgranges P, et al. Overexpression of transforming growth factor-beta1 stabilizes already-formed aortic aneurysms: a first approach to induction of functional healing by endovascular gene therapy. *Circulation* 2005;112:1008-15.
34. Xu R, Bi C, Song J, Wang L, Ge C, Liu X, et al. Upregulation of miR-142-5p in atherosclerotic plaques and regulation of oxidized low-density lipoprotein-induced apoptosis in macrophages. *Mol Med Rep* 2015;11:3229-34.
35. Wang M, Sampson ER, Jin H, Li J, Ke QH, Im HJ, et al. MMP13 is a critical target gene during the progression of osteoarthritis. *Arthritis Res Ther* 2013;15:R5.
36. Xu N, Zhang L, Meisgen F, Harada M, Heilborn J, Homey B, et al. MicroRNA-125b down-regulates matrix metalloproteinase 13 and inhibits cutaneous squamous cell carcinoma cell proliferation, migration, and invasion. *J Biol Chem* 2012;287:29899-908.
37. Goettsch C, Rauner M, Pacyna N, Hempel U, Bornstein SR, Hofbauer LC. miR-125b regulates calcification of vascular smooth muscle cells. *Am J Pathol* 2011;179:1594-600.
38. Zhang Y, Xie RL, Croce CM, Stein JL, Lian JB, van Wijnen AJ, et al. A program of microRNAs controls osteogenic lineage progression by targeting transcription factor Runx2. *Proc Natl Acad Sci U S A* 2011;108:9863-8.
39. Wang Y, Chen S, Deng C, Li F, Wang Y, Hu X, et al. MicroRNA-204 Targets Runx2 to attenuate BMP-2-induced osteoblast differentiation of human aortic valve interstitial cells. *J Cardiovasc Pharmacol* 2015;66:63-71.
40. Bastow ER, Byers S, Golub SB, Clarkin CE, Pitsillides AA, Fosang AJ. Hyaluronan synthesis and degradation in cartilage and bone. *Cell Mol Life Sci* 2008;65:395-413.

Submitted Aug 23, 2016; accepted Dec 12, 2016.

Additional material for this article may be found online at [www.jvascsurg.org](http://www.jvascsurg.org).

#### APPENDIX FILE 1 (online only).

**miR-33a-5p potential targets genes.** TargetScan targets list: [http://www.targetscan.org/cgi-bin/targetscan/vert\\_71/targetscan.cgi?species=Human&gid=&mir\\_sc=&mir\\_c=&mir\\_nc=&mir\\_vnc=&mirg=hsa-miR-33a-5p](http://www.targetscan.org/cgi-bin/targetscan/vert_71/targetscan.cgi?species=Human&gid=&mir_sc=&mir_c=&mir_nc=&mir_vnc=&mirg=hsa-miR-33a-5p)  
PicTar targets list: [http://pictar.mdc-berlin.de/cgi-bin/PicTar\\_vertibrate.cgi](http://pictar.mdc-berlin.de/cgi-bin/PicTar_vertibrate.cgi)  
miRTarBase targets list: <http://mirtarbase.mbc.nctu.edu.tw/php/search.php>

#### APPENDIX FILE 2 (online only).

**miR-99b-5p potential targets genes.** TargetScan targets list: [http://www.targetscan.org/cgi-bin/targetscan/vert\\_70/targetscan.cgi?species=Human&gid=&mir\\_sc=&mir\\_c=&mir\\_nc=&mirg=miR-99b-5p](http://www.targetscan.org/cgi-bin/targetscan/vert_70/targetscan.cgi?species=Human&gid=&mir_sc=&mir_c=&mir_nc=&mirg=miR-99b-5p)  
PicTar targets list: [http://pictar.mdc-berlin.de/cgi-bin/PicTar\\_vertibrate.cgi](http://pictar.mdc-berlin.de/cgi-bin/PicTar_vertibrate.cgi)  
miRTarBase targets list: [http://mirtarbase.mbc.nctu.edu.tw/php/search.php?org=hsa&opt=mirna\\_id&kw=miR-99b-5p&miFam=0](http://mirtarbase.mbc.nctu.edu.tw/php/search.php?org=hsa&opt=mirna_id&kw=miR-99b-5p&miFam=0)

#### APPENDIX FILE 3 (online only).

**miR-125b-5p potential targets genes.** TargetScan targets list: [http://www.targetscan.org/cgi-bin/targetscan/vert\\_70/targetscan.cgi?species=Human&gid=&mir\\_sc=&mir\\_c=&mir\\_nc=&mirg=miR-125b-5p](http://www.targetscan.org/cgi-bin/targetscan/vert_70/targetscan.cgi?species=Human&gid=&mir_sc=&mir_c=&mir_nc=&mirg=miR-125b-5p)  
PicTar targets list: [http://pictar.mdc-berlin.de/cgi-bin/PicTar\\_vertibrate.cgi](http://pictar.mdc-berlin.de/cgi-bin/PicTar_vertibrate.cgi)  
miRTarBase targets list: <http://mirtarbase.mbc.nctu.edu.tw/php/search.php>

#### APPENDIX FILE 4 (online only).

**miR-142-5p potential targets genes.** TargetScan targets list: [http://www.targetscan.org/cgi-bin/targetscan/vert\\_70/targetscan.cgi?species=Human&gid=&mir\\_sc=&mir\\_c=&mir\\_nc=&mirg=miR-142-5p](http://www.targetscan.org/cgi-bin/targetscan/vert_70/targetscan.cgi?species=Human&gid=&mir_sc=&mir_c=&mir_nc=&mirg=miR-142-5p)  
PicTar targets list: [http://pictar.mdc-berlin.de/cgi-bin/PicTar\\_vertibrate.cgi](http://pictar.mdc-berlin.de/cgi-bin/PicTar_vertibrate.cgi)  
miRTarBase targets list: <http://mirtarbase.mbc.nctu.edu.tw/php/search.php>

#### APPENDIX FILE 5 (online only).

**miR-204 potential targets genes.** TargetScan targets list: [http://www.targetscan.org/cgi-bin/targetscan/vert\\_70/targetscan.cgi?species=Human&mir\\_sc=miR-204-5p/211-5p](http://www.targetscan.org/cgi-bin/targetscan/vert_70/targetscan.cgi?species=Human&mir_sc=miR-204-5p/211-5p)  
PicTar targets list: [http://pictar.mdc-berlin.de/cgi-bin/PicTar\\_vertibrate.cgi](http://pictar.mdc-berlin.de/cgi-bin/PicTar_vertibrate.cgi)  
miRTarBase targets list: <http://mirtarbase.mbc.nctu.edu.tw/php/search.php>

#### APPENDIX FILE 6 (online only).

**miR-486-5p potential targets genes.** TargetScan targets list: [http://www.targetscan.org/cgi-bin/targetscan/vert\\_70/targetscan.cgi?species=Human&gid=&mir\\_sc=&mir\\_c=&mir\\_nc=&mirg=miR-486-5p](http://www.targetscan.org/cgi-bin/targetscan/vert_70/targetscan.cgi?species=Human&gid=&mir_sc=&mir_c=&mir_nc=&mirg=miR-486-5p)  
PicTar targets list: Not in the database.  
miRTarBase targets list: [http://mirtarbase.mbc.nctu.edu.tw/php/search.php?org=hsa&opt=mirna\\_id&kw=miR-486-5p&miFam=0](http://mirtarbase.mbc.nctu.edu.tw/php/search.php?org=hsa&opt=mirna_id&kw=miR-486-5p&miFam=0)

**Supplementary Table I (online only).** Sequences of microRNA (*miRNA*) oligonucleotides

| miRNA             | Primer sequence                | Efficiency in tissue |
|-------------------|--------------------------------|----------------------|
| cel-miR-39        | TCA CCG GGT GTA AAT CAG CTT G  | ...                  |
| hsa-miR-16        | TAG CAG CAC GTA AAT ATT GGC G  | ...                  |
| hsa-miR-33a-5p    | GTG CAT TGT AGT TGC ATT GCA    | 1.90                 |
| hsa-miR-99b-5p    | CAC CCG TAG AAC CGA CCT TGC G  | 1.88                 |
| hsa-miR-103a-2-5p | AGC TTC TTT ACA GTG CTG CCT TG | ...                  |
| hsa-miR-125b-5p   | TCC CTG AGA CCC TAA CTT GTG A  | 2.06                 |
| hsa-miR-142-5p    | CAT AAA GTA GAA AGC ACT ACT    | 1.99                 |
| hsa-miR-204-5p    | TTC CCT TTG TCA TCC TAT GCC T  | 2.05                 |
| hsa-miR-206       | TGG AAT GTA AGG AAG TGT GTG GG | ...                  |
| hsa-miR-374b-5p   | ATA TAA TAC AAC CTG CTA AGT G  | ...                  |
| hsa-miR-486-5p    | TCC TGT ACT GAG CTG CCC CGA G  | 1.98                 |

**Supplementary Table II (online only).** Validation of quantitative polymerase chain reaction (*qPCR*) array by real-time *qPCR*<sup>a</sup>

| Variable                 | qPCR array A+/A0     | Real time qPCR A+/A0 |
|--------------------------|----------------------|----------------------|
| miR-33a-5p               | 2.72                 | 2.06                 |
| miR-99b-5p               | -3.93                | -2.5                 |
| miR-103a-2-5p            | 2.42                 | 1.57                 |
| miR-125b-5p              | -2.23                | -3.71                |
| miR-142-5p               | 2.05                 | 4.16                 |
| miR-204-5p               | -1.99                | -2.84                |
| miR-206                  | -3.20                | -1.29                |
| miR-374b-5p              | 2.92                 | -2.51                |
| miR-486-5p               | -2.15                | -2.33                |
| Correlation <sup>b</sup> | Pearson $r = 0.87^c$ |                      |

A+, Aneurysm shows positive [<sup>18</sup>F]fluorodeoxyglucose uptake; A0, no aneurysm [<sup>18</sup>F]fluorodeoxyglucose uptake.

<sup>a</sup>Results are expressed as mean of fold-change between A+ and A0 pools for qPCR array and mean of fold-change between 22 A+ and 35 A0 samples for real time qPCR.

<sup>b</sup>Correlation between both techniques was performed using the Pearson linear regression curve.

<sup>c</sup> $P < .01$ .



**Supplementary Table III (online only).** Pathways potentially modulated by micro RNAs (*miRNAs*)

| miRNA       | Pathway name  | P value Bonferroni | Genes from input |
|-------------|---|--------------------|------------------|
| miR-33a-5p  | Developmental biology                                     | 4.760E-6           | 36               |
| miR-33a-5p  | TGF- $\beta$ receptor signaling pathway                   | 2.274E-5           | 20               |
| miR-33a-5p  | SREBF and miR33 in cholesterol and lipid homeostasis      | 5.606E-4           | 7                |
| miR-33a-5p  | BDNF signaling pathway                                    | 1.129E-3           | 17               |
| miR-33a-5p  | Circadian clock   | 5.537E-3           | 10               |
| miR-33a-5p  | $\alpha$ 6- $\beta$ 4 integrin signaling pathway          | 6.645E-3           | 11               |
| miR-33a-5p  | RORA activates circadian expression                       | 7.126E-3           | 7                |
| miR-33a-5p  | Signaling events mediated by HGFR (c-Met)                 | 8.821E-3           | 11               |
| miR-33a-5p  | BMP receptor signaling                                    | 9.715E-3           | 8                |
| miR-33a-5p  | PPARA activates gene expression                           | 1.139E-2           | 14               |
| miR-33a-5p  | Regulation of lipid metabolism by PPAR- $\alpha$          | 1.525E-2           | 14               |
| miR-33a-5p  | Signaling events mediated by VEGFR1 and VEGFR2            | 1.665E-2           | 10               |
| miR-33a-5p  | Axon guidance   | 3.132E-2           | 21               |
| miR-33a-5p  | c-Jun N-terminal kinases MAPK signaling                   | 3.363E-2           | 7                |
| miR-33a-5p  | Adipogenesis  | 4.115E-2           | 14               |
| miR-33a-5p  | Trk receptor signaling mediated by PI3K and PLC- $\gamma$ | 4.201E-2           | 7                |
| miR-33a-5p  | N-cadherin signaling events                               | 5.202E-2           | 7                |
| miR-125b-5p | MAPK signaling pathway                                    | 6.21E-03           | 36               |
| miR-125b-5p | HIF-1- $\alpha$ transcription factor network              | 1.37E-02           | 15               |
| miR-125b-5p | MAPKinase signaling pathway                               | 3.63E-02           | 17               |
| miR-125b-5p | JNK MAPK pathway  | 4.07E-02           | 11               |
| miR-125b-5p | Direct p53 effectors                                      | 4.13E-02           | 22               |
| miR-125b-5p | BDNF signaling pathway                                    | 4.25E-02           | 23               |
| miR-142-5p  | Developmental biology                                     | 4.29E-06           | 47               |
| miR-142-5p  | TGF- $\beta$ receptor signaling                           | 4.21E-05           | 14               |
| miR-142-5p  | Pathways in cancer  | 1.89E-04           | 37               |
| miR-142-5p  | BMP receptor signaling                                    | 3.91E-03           | 10               |
| miR-142-5p  | Ubiquitin mediated proteolysis                            | 1.43E-02           | 19               |
| miR-142-5p  | TGF- $\beta$ receptor signaling activates SMADs           | 1.50E-02           | 9                |
| miR-142-5p  | TGF- $\beta$ signaling pathway                            | 1.56E-02           | 15               |
| miR-142-5p  | Axon guidance   | 2.08E-02           | 28               |
| miR-142-5p  | Colorectal cancer   | 2.31E-02           | 12               |
| miR-204-5p  | Axon guidance   | 1.18E-03           | 29               |
| miR-204-5p  | BDNF signaling pathway                                    | 2.05E-03           | 20               |
| miR-204-5p  | Axon guidance   | 5.26E-03           | 18               |
| miR-204-5p  | Leptin signaling pathway                                  | 6.56E-03           | 12               |
| miR-204-5p  | SIDS susceptibility pathways                              | 1.08E-02           | 20               |
| miR-204-5p  | Signaling events mediated by VEGFR1 and VEGFR2            | 1.12E-02           | 12               |
| miR-204-5p  | Netrin-1 signaling  | 1.29E-02           | 10               |
| miR-204-5p  | Hippo signaling pathway                                   | 2.23E-02           | 19               |

BDNF, Brain-derived neurotrophic factor; BMP, bone morphogenetic protein; HGFR, hepatocyte growth factor receptor; HIF-1, hypoxia-inducible factor 1; JNK, c-Jun N-terminal kinase; MAPK, mitogen-activated protein kinase; PI3K, phosphatidylinositol-3-kinases; PLC, phospholipase C; PPARA, peroxisome proliferator-activated receptor- $\alpha$ ; RORA, RAR-related orphan receptor A; SIDS, sudden infant death syndrome; SREBF, sterol regulatory element-binding factor; TGF, transforming growth factor; VEGFR, vascular endothelial growth factor receptor.